Towards Consistent Color Image Acquisition in Dermatology

Yves Vander Haeghen*,***, Prof. Dr. J.M. Naeyeart**, Prof. Dr. I. Lemahieu*
* Dept. Engineering, ELIS-MEDISIP, University Gent, St.-Pietersnieuwstraat 41, 9000 Gent, Belgium
** Dept. Dermatology, University Hospital, De Pintelaan 185, 9000 Gent, Belgium
***E-mail: Yves.VanderHaeghen@rug.ac.be

Abstract— **We propose a simple, quick and practical color calibration procedure that results in a precise (reproducible), albeit not very accurate (close to values obtained with a reference device), color description in a standard device-dependent color space (sRGB). The system consists of a 3-chip CCD camera, a continuous ring-light, frame grabber and PC. The calibration procedure involves building a profile of the acquisition system based on the 24 color targets. This profile is easily checked before a set of image acquisitions and remains valid over a long period. The acquired images are transformed from the device-dependent RGB camera space to the gamma corrected sRGB (or ITU-R BT.709) space and are readily displayable on a CRT-based monitor. Moreover, sRGB tristimulus values are readily transformed the CIE L*a*b* space, allowing percetual color differences ΔE^*_{ab} to be computed. The field of view (FOV) of the system is 1.5 by 2.0 cm, and the resolution is around 38 pixels/mm for a 570 by 760 pixel image. Although the accuracy of the proposed procedure is not very high ($\Delta E^*_{ab} > 10$ for some of the MBCCC targets), the precision or reproducibility for those targets is quite good with an average error of $\langle \Delta E^*_{ab} \rangle = 0.34$, and a maximal error of $\Delta E^*_{ab} < 1.2$. For in vivo measurements typical maximal error is more like $\Delta E^*_{ab} < 2.2$ based on preliminary findings, mainly because of the difficulty in determining consistent regions of intrest (ROI's) in different images.**

Keywords— **Color calibration, Dermatology, Color image acquisition, camera calibration, CCD camera**

I. Introduction

In dermatology color and color difference often convey important diagnostic information, especially when investigating pigmented lesions and more particularly skin cancer. In order to make quantitative color measurements on irregular and variable sized skin lesions, standard chromameters or spectrophotometers are generally useless because of their fixed aperture. Traditional photography has the benefit of having a visual record of the lesion, but doesn't have very consistent color reproduction due to differences in film, illumination and development. Although in digital photography no film is involved, it not straightforward to obtain a constant response from a digital image acquisition system [1], [2]. Moreover, most digital cameras are not colorimetric, i.e. their color sensors don't have spectral response functions that are proportional to the CIE $\bar{x}\,\bar{y}\,\bar{z}$ color matching functions (CIE stands for 'Commission Internationale de l'Eclairage', a standardizing body in the field of color science). This means it is not easy to compute perceptual color differences because the relation between the device-dependent camera RGB space and the device-independent CIE XYZ space is unknown and has to be determined. This subject was already extensively covered in the literature [3], [4], [2], [5], [6], [7], [8], [9], but here the emphasis is clearly on a simple and practical scheme, making no pretense at being a color appearance model or at color constancy. Instead it avoids some of the problems concerning changes in illuminant between source (camera RGB) and output space (sRGB). The use of digital photography in dermatology has already been investigated several times, mostly using device-dependent color spaces, e.g. RGB and HSV [10], [11], [12], [13]. Sometimes device-independent color spaces were used [14], although it is unclear just how the necessary transform was obtained. At present no system for use in dermatology has been proposed that uses a standard color space with known primaries and white point. Such a color space has the additional benefit of allowing the interchange of images for more than just viewing purposes, and opens perspectives in the area of telemedicine.

II. The acquisition system

The acquisition system consists of a JVC KY-55B 3-chip CCD camera with a Pentax manual zoom lens, a Schott[1] KL1500 150 Watt halogen light source and an Integral Technologies[2], FlashPoint 128 frame grabber. The field of view of the CCD camera is 2.0 cm by 1.5 cm. With an image containing 760 by 570 pixels the resolution is 38 pixels/mm. The light source is linked by a 2 m long optical fiber to a continuous ring-light that fits around the zoom lens. A blue filter changes the color temperature of the light source from 2800 K to around 5100 K. The frame grabber is fitted in a standard 150

[1]Shott Glaswerke, Hagenauer strasze 38, D-65203 Wiesbaden
[2]Integral Technologies, Inc, 9855 Crosspoint blvd, Suite 126, Indianapolis, Indiana, 46256 USA

MHz Pentium PC running Windows 95, and acquisition is done using the PAL analog RGB format which is digitized with 8-bit precision per color channel. The settings of the CCD camera can be adjusted through the serial port of the PC. The settings of the frame grabber are controlled using the FlashPoint Software Developer's Toolkit 3.0 from Integral Technologies. The color targets are taken from the MacBeth Color Checker Chart[3] (MBCCC).

III. Calibration of acquisition system

The calibration of the whole acquisition system consists of several consecutive steps: determination of the camera offset, the frame grabber offset, the frame grabber gain, the camera aperture, the color gains of the camera, the linearizing look-up table, and finally the transform from the device-dependent RGB space to the device-independent CIE XYZ space. All these settings are stored in a so-called profile of the acquisition system. An important issue in these steps, besides consistency in time, is to maximize the dynamic range of the camera and frame grabber. This means that for a perfectly diffuse reflector and given a certain illuminant the camera RGB output voltages should be at their maximum, and the corresponding digitized values should be $(255, 255, 255)$. We also have to make sure that a perfectly dark scene should result in zero output voltages at the camera and digitized values of $(0, 0, 0)$. Any non-linearity of acquisition system (mainly the camera sensors) with regard to luminance is removed using a look-up table (LUT). For more details and the individual calibration steps, see [15].

The RGB to XYZ transform is determined by a least-squares method based on measurements of the MBCCC targets with known XYZ tristimuli. It is clear that minimizing the mapping errors in a more perceptual color space, e.g. R*G*B* or CIE L*a*b*, would be far better, but this means tackling non-linear optimization in a multidimensional space. Properly mapping neutral color is very important for proper color reproduction, see [16], and thus the white-point preserving transformation proposed in [6] performs very well, especially under maximum ignorance assumptions. However, as the proportion of neutral color targets used in determining T is quite large there will be a 'natural' bias in the least-squares procedure towards properly mapping neutral colors. Moreover, the maximum ignorance assumption may not be the best premise in the case of skin imaging.

[3]Macbeth, 405 Little Britain rd, New Windsor, NY 12553-6148, USA

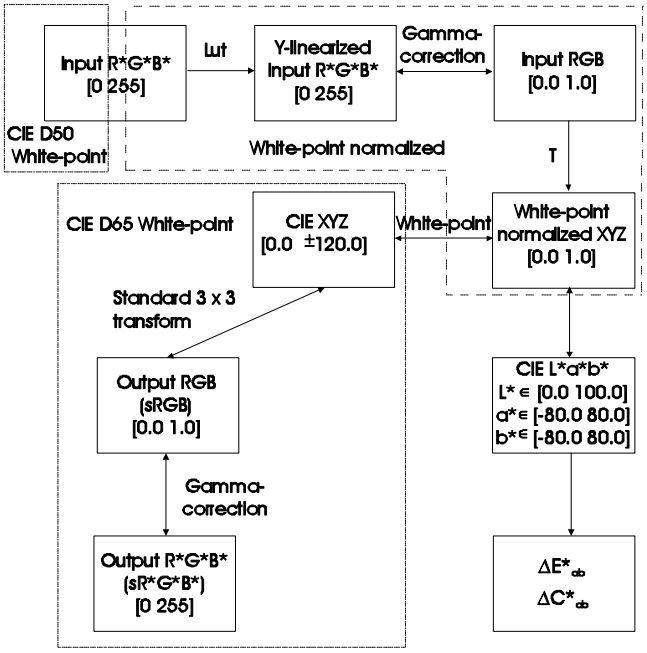

Fig. 1. The different color spaces of the calibration scheme and their relations.

IV. Checking and adjusting an existing acquisition system calibration profile

Once a profile is determined and stored it can be used as long as the acquisition system doesn't change too much (aging of the light source bulb, changes in camera sensor spectral response, ...). This is easily checked by comparing the CIE L*a*b* value of a test target (MBCCC 'white') with its value during the calibration procedure. We set a limit of $1\,\Delta E^*_{ab}$ unit as the maximum deviation for the acceptance of the profile, as this is generally accepted to be lowest visable perceptual color difference. Images acquired with a validated and adjusted profile are transformed to the gamma corrected sRGB space (sR*G*B*) before they are stored, see fig. 1 and fig. 5 for an example. This is called output rendering and should provide a fairly realistic image on any modern CRT-based monitor which has its white-point set at 6500 K [17].

V. Experimental results and discussion

With accuracy we mean the consistency with which measurements of colors are close their real measured values, as measured by a reference instrument, e.g. a spectrophotometer. Good accuracy will be especially important when exchanging images. Experiments consisted of 19 measurements of the MBCCC targets under different profiles and after different warmup-times of the acquisition system. For each target t the average error $\langle \Delta E^*_{ab}(t) \rangle$ was computed with regard to the real CIE L*a*b* value of the target, see fig. 2. Two conclusions

present themselves: firstly, the RGB to CIE XYZ transform does indeed perform well for neutral colors (targets 19 to 24), and secondly, the greatly varying results between the targets indicates that, as expected, the minimization of mapping errors in the CIE XYZ space is not such a good idea. Averaged over all the MBCCC targets we get $\langle \Delta E^*_{ab} \rangle = 4.1$ with $\Delta E^*_{ab} < 12$. It has to be noted that proper accuracy measurements should use other targets than the ones used in the determination of the acquisition system profile. Real accuracy may therefore be lower than presented here. With precision we describe the reproducibility of measurements, or the way repeated measurements are spreaded around the average of those measurements. Precision will be important for any quantitative measurement of image color characteristics. We can distinguish several types of precision: short-term precision when making several consecutive measurements of the same target, medium-term or profile precision when comparing measurements made under one profile, and long-term or inter-profile precision when talking about the agreement between measurements made under different profiles.

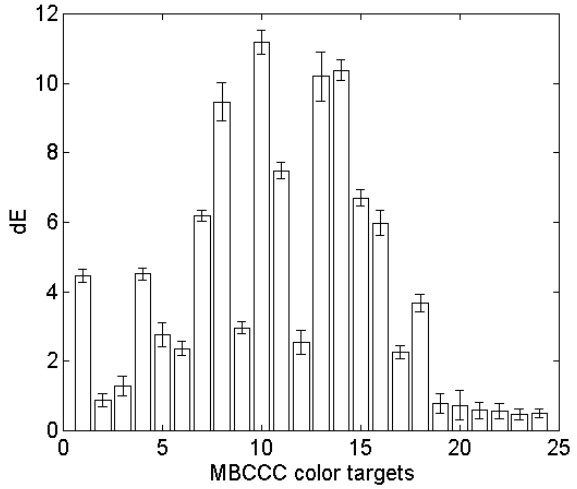

Fig. 2. The average accuracy of the MBCCC color targets. The error bars represent one sample standard deviation

Short term precision based on 20 consecutive measurements of the MBCCC 'white' target was very good: $\langle \Delta E^*_{ab}(white) \rangle = 0.04$, with $\Delta E^*_{ab}(white) < 0.1$. The results for the medium-term and long-term precision can be seen in fig. 3 and 4. Here the average error $\langle \Delta E^*_{ab}(t) \rangle$ for each target t was computed with regard to the average sample CIE L*a*b* value of the target (10 and 9 measurements respectively). To simulate possible long-term changes in the acquisition system, the color temperature of the light source was modified for half of the profiles of fig. 4. There was no noticeable difference in precision between profiles for the normal and modified acquisition system. The average, sample standard deviation and maximal perceptual color differences over all the MBCCC targets for medium-term and long-term precision are $\langle \Delta E^*_{ab} \rangle = 0.34$, $sE^*_{ab} = 0.094$ with $\Delta E^*_{ab} < 1.2$, and $\langle \Delta E^*_{ab} \rangle = 0.30$, $s_{E^*_{ab}} = 0.10$ with $\Delta E^*_{ab} < 1.2$ respectively. Finally, 4 measurements of the same area of human skin were made: the first two with the same acquisition system profile and during the same warm-up cycle, the third on a different warm-up cycle, and the fourth using a newly created profile. Because it is very difficult to obtain a pixel-precise alignment of the acquired images, average CIE L*a*b* values

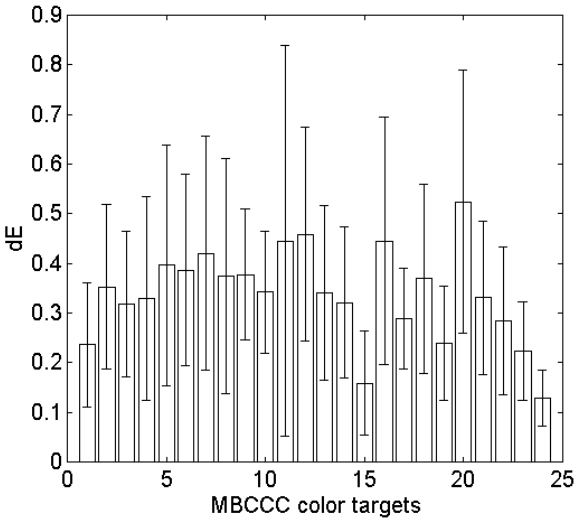

Fig. 3. The average medium-term precision of the MBCCC color targets. The error bars represent one sample standard deviation

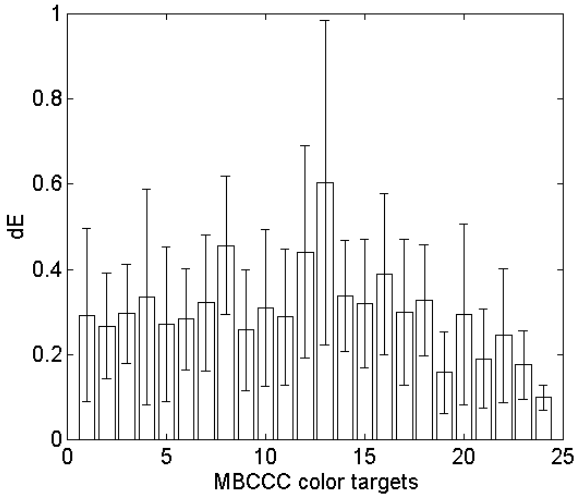

Fig. 4. The average long-term precision of the MBCCC color targets. The error bars represent one sample standard deviation

	$\langle L*a*b* \rangle$	s_{L*a*b*}
MBCCC	(94.49, -0.26, 0.22)	
Calib Im1, Im2,Im3	(94.95, -0.28, -0.53)	
Calib Im4	(94.86, -0.18, -0.60)	
Im1:White	(92.16, -0.25, -1.26)	(0.47, 0.89, 0.72)
Im2:White	(92.22, -0.14, -1.3)	(0.45, 0.88, 0.69)
Im3:White	(91.92 -0.12, -1.12)	(0.49, 0.94, 0.76)
Im4:White	(92.11 -0.12, -1.05)	(0.43, 0.81, 0.66)
Im1:Flesh	(70.52, 10.87, 8.56)	(3.35, 2.23, 3.27)
Im2:Flesh	(70.80, 10.32, 8.72)	(3.44, 1.99, 2.81)
Im3:Flesh	(72.47, 7.54, 8.88)	(3.20, 1.94, 2.79)
Im4:Flesh	(70.95, 8.37, 10.75)	(3.24, 1.83, 2.47)
Im1:Naevus	(45.94, 23.72, 19.24)	(8.21, 5.70, 6.78)
Im2:Naevus	(46.83, 23.26, 19.45)	(7.80, 5.41, 6.39)
Im3:Naevus	(47.03, 21.30, 20.58)	(7.74, 5.65, 6.45)
Im4:Naevus	(48.25, 21.36, 21.59)	(7.71, 5.15, 5.69)

TABLE I
The average CIE L*a*b* values of the different regions in the 4 images and their sample standard deviations. The first 3 lines are the real and the values at calibration of the white target included in the skin images.

were compaired over three roughly feature-wise equal regions of intrest (ROI's) of the different images. These ROI's are labeled 'naevus', 'flesh' and 'white', see fig. 5. The 'white' ROI is equal to one of the MBCCC targets, and therefore its theoretical L*a*b* value as well as its value during both calibrations, once for image 1 to 3 and once for image 4, is known. The results of these measurements can be seen in table I. The standard deviation is based on the sample variance-covariance matrix of the CIE L*a*b* values of the pixels in each ROI. As such it is a measure of how well the ROI can be represented by an average value, and concurrently of possible errors when compairing these average values due to ROI mismatches in the different images, e.g. due to the diffuse nature of the border of the 'naevus' ROI. Table II shows the values in table I averaged over the 4 images. The 'white' ROI yields very reproducible results, and with a color difference of the same order as in fig. 4. The fact that the lightness L* is a little low is probably due to the fact that the target was not measured in the center of the images. This indicates a non-uniformity in the lightsource which can easily be corrected in future using an image of the 'white' target. The other 2 ROI's result in standard deviations which are still small compaired to those in table I, and in $\Delta E^*_{ab} < 2.2$. This means that with a little care in the selection of the ROI's it must be possible to make quite precise and repeated colorimetric measurements of certain skin areas. It is clear that these are preliminary findings, and that more in vivo measurements have to be made, especially concerning the long-term follow-up (months, even years) of certain skin areas, e.g. melanocytic naevi in patients with an increased probability of malignant melanoma.

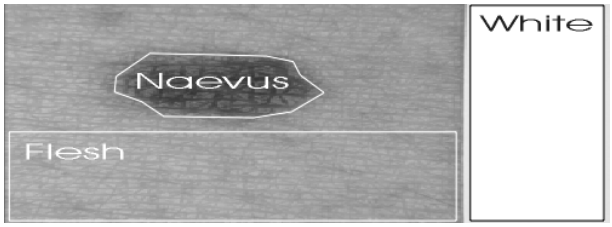

Fig. 5. The skin image and the ROI's used in the computations

	$\langle L*a*b* \rangle$	s_{L*a*b*}
White	(92.10, -0.16, -1.19)	(0.13, 0.06, 0.13)
Flesh	(71.69, 9.28, 9.23)	(1.21, 1.58, 1.02)
Naevus	(49.01, 22.41, 20.21)	(0.95, 1.26, 1.09)
	$\langle \Delta E^*_{ab} \rangle$	$Max(\Delta E^*_{ab})$
White	0.16	0.20
Flesh	1.60	2.13
Naevus	1.91	2.18

TABLE II
The average CIE L*a*b* values over the 4 images in table I, their sample standard deviations and the average and maximal percepual color difference.

VI. Conclusions

We have proposed a color calibration procedure which allows colorimetrically consistent acquisition of digital images. These images are stored in a standard color space with known primaries and white-point, and as such can be exchanged and compaired with other images in the same color space, even if acquired by other means. They are readily displayable on CRT-based displays. The feasability of making quite precise and repeated colorimetric measurements of certain skin areas has been demonstrated, and will be the topic of further research.

VII. Acknowledgment

This project is funded by the FWO in Belgium, ref. F7801

References

[1] G. E. Healey and R. Kondepudy, "Radiometric CCD camera calibration and noise estimation," *IEEE Transcations on Pattern Analysis and Machine Intelligence*, vol. 16, no. 3, pp. 267–276, 1994.

[2] Y.-C. Chang and J. F. Reid, "RGB calibration for color image analysis in machine vision," *IEEE Transactions on Image Processing*, vol. 5, no. 10, pp. 1414–1422, 1996.

[3] B. A. Wandell, "The synthesis and analysis of color images,"

IEEE Transactions on Pattern Analysis and Machine Intelligence, vol. PAMI-9, no. 1, pp. 2–13, 1987.

[4] D. Slater and G. Healey, "The illumination-invariant recognition of 3d objects using local color invariants," *IEEE Transactions on Pattern Analysis and Machine Intelligence*, vol. 18, no. 2, pp. 206–210, 1996.

[5] G. Finlayson, "Color in perspective," *IEEE Transactions on Pattern Analysis and Machine Intelligence*, vol. 18, no. 10, pp. 1034–1038, 1996.

[6] G. D. Finlayson and M. S. Drew, "White-point preserving color correction," in *Fifth Color Imaging Conference: Color Science, Systems and Applications*, pp. 258–261, IS&T, SID,, 1997.

[7] E. Boldrin, P. Campadelli, and R. Schettini, "Learning colkor appearance models," in *Fifth Color Imaging Conference: Color Science, Systems and Applications*, pp. 173–176, IS&T, SID,, 1997.

[8] P. M. Hubel, J. Holm, G. D. Finlayson, and M. S. Drew, "Matrix calculations for digital photography," in *Fifth Color Imaging Conference: Color Science, Systems and Applications*, pp. 105–111, IS&T, SID,, 1997.

[9] H. Kang, *Color Technology for Electronic Imaging Devices*. SPIE Optical Engineering Press, 1997.

[10] N. Cascinelli et al., "A possible tool for clinical diagnosis of melanoma: The computer," *Journal of the American Academy of Dermatology*, vol. 16, no. 2, Part 1, pp. 361–367, 1987.

[11] J. L. Stone, R. L. Peterson, and J. E. Wolf, "Digital imaging techniques in dermatology," *Journal of the American Academy of Dermatology*, no. 5, part 1, pp. 913–917, 1990.

[12] R. Kenet et al., "Clinical diagnosis of pigmented lesions using digital epiluminescence microscopy," *Arch. of Dermatology*, vol. 129, pp. 157–174, 1993.

[13] W. Stolz et al., "Improvement of monitoring of melanocytic skin lesions with the use of a computerized acquisition and surveilland with a skin surface microscopic television camera," *Journal of the American Academy of Dermatology*, vol. 35, no. 2, Part 1, pp. 202–207, 1996.

[14] T. Schindewolf et al., "Evaluation of different image acquisition techniques for a computer vision system in the diagnosis of malignant melanoma," *Journal of the American Academy of Dermatology*, vol. 31, no. 1, pp. 33–41, 1994.

[15] Y. Vander Haeghen et al., "Consistent digital color image acquisition of the skin," in *In review: EMBSC 98, Oct.-Nov., Hong Kong*, EMBS, 1998.

[16] R. Hunt, *The Reproduction of Colour*. Fountain Press, fifth edition ed., 1995.

[17] J. Holm, "Issues relating to the transformation of sensor data into standard color spaces," in *Fifth Color Imaging Conference: Color Science, Systems and Applications*, pp. 290–295, IS&T, SID,, 1997.